Molecular Biology of the Cell
Vol. 15, 1557–1567, April 2004

Association with Membrane Protrusions Makes ErbB2 an Internalization-resistant Receptor

Anette M. Hommelgaard, Mads Lerdrup, and Bo van Deurs*

Structural Cell Biology Unit, Department of Medical Anatomy, The Panum Institute, University of Copenhagen, Copenhagen 2200 N, Denmark

Submitted August 15, 2003; Revised December 10, 2003; Accepted December 22, 2003
Monitoring Editor: Howard Riezman

In contrast to the epidermal growth factor (EGF) receptor, ErbB2 is known to remain at the plasma membrane after ligand binding and dimerization. However, why ErbB2 is not efficiently down-regulated has remained elusive. Basically, two possibilities exist: ErbB2 is internalization resistant or it is efficiently recycled after internalization. By a combination of confocal microscopy, immunogold labeling electron microscopy, and biochemical techniques we show that ErbB2 is preferentially associated with membrane protrusions. Moreover, it is efficiently excluded from clathrin-coated pits and is not seen in transferrin receptor-containing endosomes. This pattern is not changed after binding of EGF, heregulin, or herceptin. The exclusion from coated pits is so pronounced that it cannot just be explained by lack of an internalization signal. Although ErbB2 is a raft-associated protein, the localization of ErbB2 to protrusions is not a result of raft binding. Also, an intact actin cytoskeleton is not required for keeping ErbB2 away from coated pits. However, after efficient cross-linking, ErbB2 is removed from protrusions to occur on the bulk membrane, in coated pits, and in endosomes. These data show that ErbB2 is a remarkably internalization-resistant receptor and suggest that the mechanism underlying the firm association of ErbB2 with protrusions also is the reason for this resistance.

INTRODUCTION

ErbB2, a member of the epidermal growth factor (EGF) receptor (EGFR) family, has no specific ligand, but it is the main heterodimerization partner for the other family members (Sliwkowski *et al*., 1994; Yarden, 2001; Yarden and Sliwkowski, 2001). The dimerization is mediated by a unique dimerization arm localized to the extracellular (N-terminal) portion of the receptor. Whereas exposure of this arm normally requires ligand binding and reorganization of the exterior portion of ErbB receptors, it is constitutively exposed in ErbB2 (Burgess *et al*., 2003). Moreover, in contrast to the EGFR, which is rapidly down-regulated upon ligand stimulation (Sorkin and Von Zastrow, 2002), ErbB2 avoids delivery to lysosomes and subsequent proteolysis and has a long half-life at the plasma membrane (Gilboa *et al*., 1995; Baulida *et al*., 1996; Baulida and Carpenter, 1997; Waterman *et al*., 1998; Wang *et al*., 1999). ErbB2 expression is up-regulated in various cancers. For instance, 20–30% of breast cancers show strong overexpression, and this correlates with poor prognosis (Slamon *et al*., 1989; Reese and Slamon, 1997; Eccles, 2001). The oncogenic potential of ErbB2 may in part be explained by its capability to avoid down-regulation together with its pronounced engagement in formation of heterodimers. When overexpressed, ErbB2 causes the other family members to escape the lysosomal pathway upon ligand binding and receptor activation (Yarden, 2001). However, the reason why ErbB2 escapes the lysosomal pathway and remains at the plasma membrane has remained elusive. Basically, two mechanisms could lead to retention of ErbB2 at the plasma membrane: either ErbB2 somehow avoids internalization or it becomes efficiently recycled from endosomes to the plasma membrane after internalization. In a study with EGFR and ErbB2 chimeric receptors, it was proposed that the cytoplasmic tail of ErbB2 did not have an internalization signal or it contained an inhibitory signal for efficient clathrin-mediated endocytosis (Sorkin *et al*., 1993). Studies with EGFR-ErbB2/3/4 chimeras revealed that this might be true for ErbB3 and ErbB4 as well (Baulida *et al*., 1996). Moreover, cell fractionation studies indicated that ErbB2 heterodimers were not delivered to endosomes (Wang *et al*., 1999). In contrast, EM studies have suggested that ErbB2 becomes internalized by clathrin-coated vesicles like many other receptors (Hurwitz *et al*., 1995; Maier *et al*., 1991), and the predominant opinion has been that ErbB2 heterodimers are recycled from endosomes to the plasma membrane after internalization, thereby avoiding the ubiquitin-cCbl-mediated lysosomal pathway that the EGFR homodimers follow (Lenferink *et al*., 1998; Klapper *et al*., 2000; Yarden, 2001; Citri *et al*., 2003). Recent mathematical modeling of ErbB2 trafficking has been interpreted in favor of decreased internalization and increased recycling of ErbB2 (Hendriks *et al*., 2003a,b). Herceptin or trastuzumab, a humanized monoclonal antibody (mAb) against ErbB2, which is widely used in treatment of breast cancer, is generally believed to exert its antitumor effect by driving internalized ErbB2 away from the recycling pathway and toward the lysosomal degradative pathway (Rubin and Yarden, 2001; Yarden, 2001; Menard *et al*., 2003). However, other mechanisms of herceptin action that do not require ErbB2 internalization have also been proposed, such as prevention of heterodimerization (Klapper *et al*., 1997) and protection of the receptor against proteolysis in vivo and thereby a decrease in the number of cleaved ErbB2 fragments that are constitutive active (Molina *et al*., 2001).

We now report that in the human breast cancer cell line SKBR3, ErbB2 is preferentially and stably associated with

Article published online ahead of print. Mol. Biol. Cell 10.1091/mbc.E03–08–0596. Article and publication date are available at www.molbiolcell.org/cgi/doi/10.1091/mbc.E03–08–0596.

* Corresponding author. E-mail address: b.v.deurs@mai.ku.dk.

plasma membrane protrusions and that neither binding of EGF, heregulin, nor herceptin changes this localization or stimulates internalization of ErbB2. Only by substantial cross-linking of ErbB2 it was possible to drive ErbB2 away from the protrusions and thereby make it internalizable. It is proposed that the association of ErbB2 with protrusions is the reason why this receptor is internalization resistant.

MATERIALS AND METHODS

Cell Culture Conditions

The SKBR3 breast cancer cell line was obtained from the American Type Culture Collection (Manassas, VA). The cells were grown in T25, T75, or T150 flasks and incubated at 37°C, 5% CO_2 in DMEM supplemented with 10% fetal calf serum, 2 mM glutamine, 10 U/ml penicillin, and 10 μg/ml streptomycin (all reagents from Invitrogen, Carlsbad, CA).

Detergent Extraction and Centrifugation

Cells were plated in T75 flask and the medium changed to normal growth medium without serum the day before the experiment. Control cells were incubated with DMEM buffer (DMEM without $NaHCO_3$, with HEPES, 2 mM glutamine, and 0.2% bovine serum albumin) for 30 min at 37°C, rinsed three times with phosphate-buffered saline (PBS), and harvested in ice-cold PBS by using a rubber policeman. The cells were pelleted by centrifugation and resuspended in ice-cold lysis buffer A (50 mM Tris-HCl, pH 7.4, 150 mM NaCl, 2 mM EDTA, 10 mM NaF, 1 mM vanadate, 1% protease inhibitor cocktail; Sigma-Aldrich, St. Louis, MO) containing 1% detergent (Triton X-100 [Tx-100], Brij58, or Brij98; all from Sigma-Aldrich). The Tx-100 and Brij58 detergent extracts were gently mixed for 30 min at 4°C, and the Brij98 detergent extracts for 10 min at 37°C. The samples were centrifuged at 16,000 $\times$ *g* for 20 min at 4°C, the supernatant was collected, and the insoluble membrane domain (the pellet fraction) was washed once, recentrifuged, and resuspended in lysis buffer A containing 1% of the appropriate detergent.

In some experiments, the cells were incubated with 8 mM methyl-β-cyclodextrin (mβCD; Sigma-Aldrich), 20 μg/ml Latrunculin A (Sigma-Aldrich), 20 ng/ml heregulin-β_1 (R&D Systems, Minneapolis, MN), or 10 μg/ml herceptin (a generous gift from Dr. M. Rörth, Department of Oncology, The Finsen Center, Rigshospitalet, Copenhagen, Denmark) in DMEM-HEPES buffer for 30 min at 37°C before harvesting of the cells. The lysis buffer used contained 1% Brij98.

Laemmli buffer (62.5 mM Tris-HCl, pH 6.8, 2% SDS, 4.35% glycerol, and 0.02% bromphenol blue) with 50 mM dithiothreitol (DTT) was added to the supernatant and pellet fractions and heated for 5 min at 95°C, and then further processed for Western blotting.

Sucrose Gradient Centrifugations

Cells were treated with 8 mM mβCD in DMEM-HEPES buffer or DMEM-HEPES (control cells) for 30 min at 37°C. The cells were rinsed three times with PBS and harvested in ice-cold PBS by using a rubber policeman, followed by centrifugation (10,000 $\times$ *g* for 8 min at 4°C) to pellet the cells. The cells were resuspended in 1 ml of lysis buffer A with 1% Brij98 and incubated for 10 min at 37°C. The detergent extract was then adjusted to 40% (wt/vol) sucrose by addition of 1 ml of 80% (wt/vol) sucrose prepared in lysis buffer A, which was placed at the bottom of the centrifuge tube. A continuous 15–35% sucrose gradient was placed on top of the cell extract using a gradient mixer (SG 15; Hoeffer, San Francisco, CA). The samples were centrifuged at 35,000 rpm in a SW41 rotor (Beckman Coulter, Fullerton, CA) for 16–20 h at 3°C. After centrifugation, 1-ml fractions were collected from the bottom of the gradient (fraction number one is from the bottom of the gradient, and fraction number 12 is from the top of the gradient). The pellet fraction was resuspended in 1 ml of lysis buffer A with 1% of the appropriate detergent. Laemmli buffer with 50 mM DTT was added to the fractions, and the samples heated for 5 min at 95°C and further processed for Western blotting.

Biotin Labeling

Cells were plated in T25 flasks, and the medium was changed the day before the experiment to growth medium without serum. The cells were rinsed twice in ice-cold PBS with Ca^{2+} and Mg^{2+} (PBS-CM) for 10 min at 4°C. Sulfo-NHS-SS-Biotin (Pierce Chemical, Rockford, IL), 0.5 mg/ml, dissolved in PBS-CM was added to the cells at 4°C on a shaking table. After 20 min, additional 0.5 mg/ml Sulfo-NHS-SS-Biotin was added to the cells and further incubated at 4°C for 20 min. The cells were washed with PBS containing 10% fetal calf serum (FCS) for 10 min at 4°C. Control cells were incubated with PBS-CM containing 10% FCS for 60 min at 37°C. Some cells were incubated with either 20 ng/ml heregulin, 10 μg/ml herceptin, or the mouse mAb against ErbB2 (sc-08; Santa Cruz Biotechnology) diluted 1:100 in PBS-CM with 10% FCS for 60 min at 37°C. The cells incubated with sc-08 were washed and further incubated for 30 min at 37°C with Alexa 488-labeled goat anti-mouse (GAM-488) (Molecular Probes, Eugene, OR) diluted 1:400. The treatment was stopped by transferring the tubes back on ice, and the cells were rinsed two times with ice-cold PBS-CM with 10% FCS. The biotin on the membrane surface was removed by incubating the cells in reducing solution (50 mM glutathione [Sigma-Aldrich], 75 mM NaCl, 75 mM NaOH, and 10% FCS) for 20 min at 4°C, which was repeated once. The free SH groups were quenched in 5 mg/ml iodoacetamide (Sigma-Aldrich) in PBS-CM with 1% bovine serum albumin for 15 min at 4°C. The cells were scraped of in lysis buffer A with 1% NP-40 (Bie & Berntsen), pelleted by centrifugation, resuspended in lysis buffer A with 1% NP-40, lysed for 20 min at 4°C, and sonicated twice. The protein concentration of the samples was determined (see Protein Determination), and the samples were standardized to 0.5 μg/ml in lysis buffer A with 1% NP-40. Twenty-five microliters of streptavidin-coated beads (Sigma-Aldrich) were added to the samples for 1 h at 4°C. The cells were centrifuged for 30 s at 4°C at 16,000 $\times$ *g*, the pellet washed four times with lysis buffer A with 1% NP-40, and centrifuged at high speed for 30 s at 4°C after each wash. The pellet was dissolved in lysis buffer A with 1% NP-40. Laemmli buffer with 50 mM DTT was added to the fractions, and the samples were heated for 5 min at 95°C and further processed for Western blotting.

Western Blotting

The samples were electrophoresed on 8% Bis-Tris-acrylamide gels. After electrophoresis, the proteins were transferred to a polyvinylidene difluoride membrane (Amersham Biosciences AB, Uppsala, Sweden), and nonspecific binding sites were blocked with 5% milk powder (Bio-Rad, Hercules, CA) in PBS containing 0.1% Tween 20 (blocking buffer). Blots were probed with primary antibody in blocking buffer, followed by a horseradish peroxidase (HRP)-conjugated secondary antibody in blocking buffer. The HRP signal was detected using enhanced chemiluminescence reagents exposed to a Hyperfilm (Amersham Biosciences AB).

The antibodies used were a cocktail of two mouse monoclonal ErbB-2 antibodies (antibody-17; Neomarkers, Freemont, CA) diluted 1:3,000, rabbit polyclonal anti-ErbB2 (2242; Cell Signaling Technology, Beverly, MA) diluted 1:1,000, mouse monoclonal anti-β-actin diluted 1:10,000 (Sigma-Aldrich), rabbit polyclonal anti-caveolin-1 (BD Transduction Laboratories, Lexington, KY) diluted 1:6,000, HRP-conjugated swine anti-rabbit diluted 1:3,000 (DAKO, Carpinteria, CA), and HRP-conjugated goat anti-mouse diluted 1:2,000 (DAKO).

Cholesterol Determination

Cells were treated with 8 mM mβCD in DMEM-HEPES buffer or DMEM-HEPES (control cells) for 30 min at 37°C. After incubation, the cells were rinsed three times with PBS, harvested in ice-cold PBS, and the cells pelleted by centrifugation. The cells were lysed in lysis buffer A, and the lysate was sonicated twice (IKA Labortechnik, Staufen, Germany). The cholesterol content of the samples was determined spectrophotometrically using the Infinity Cholesterol Assay kit from Sigma-Aldrich.

Protein Determination

Protein concentrations were determined by the DC protein assay as described by the manufacturer (Bio-Rad).

Immunofluorescence Microscopy

Cells were plated on four-well chamber slices (Lab-Tek, Naperville, IL). Control cells were incubated with DMEM-HEPES buffer for 60 min at 37°C, washed with PBS, and fixed in 2% paraformaldehyde in PBS for 10 min on ice followed by 10 min at room temperature (RT). Some cells were incubated with 20 ng/ml heregulin, 10 μg/ml herceptin, or 10 ng/ml EGF (Calbiochem, San Diego, CA) in DMEM-HEPES buffer for 60 min at 37°C before fixation. Nonspecific binding was blocked, and the cell membrane was permeabilized in blocking buffer (5% goat serum [DAKO] in PBS containing 0.2% saponin) for 20 min at RT. Cells were incubated with primary antibody in blocking buffer for 1 h at RT, rinsed three times with PBS, incubated with secondary antibody or 10 μg/ml Alexa 594-labeled cholera toxin-B chain (CT-594; Molecular Probes) in blocking buffer for 30 min at RT, rinsed three times with PBS, and mounted with Flouromount G (Southern Biotechnology Associates, Birmingham, AL). The slices were examined with an LSM 510 Meta confocal microscope (Carl Zeiss, Jena, Germany), and the images were taken with the LSM software (Carl Zeiss). The pictures were further processed with Adobe Photoshop 7.0 and Adobe Illustrator 10.0.

The antibodies used were mouse monoclonal anti-ErbB2 (sc-08; Santa Cruz Biotechnology) diluted 1:200, rabbit polyclonal anti-ErbB2 (2242; Cell Signaling Technology) diluted 1:200, mouse monoclonal IgG2b anti-transferrin receptor (TfR) (309i; Novocastra, Newcastle, United Kingdom) diluted 1:10, mouse monoclonal IgG1 anti-TfR (B3/25; Chemicon International, Temecula, CA) diluted 1:100, Alexa 488-labeled goat anti-mouse (GAM-488; Molecular Probes) diluted 1:400, Alexa 488-labeled goat anti-mouse-IgG1 (Molecular Probes) diluted 1:400, Alexa 568-labeled goat anti-mouse-IgG2b (Molecular Probes) diluted 1:400, and Alexa 568-labeled swine anti-rabbit (Molecular Probes) diluted 1:400.

Electron Microscopy (EM)

Preembedding Immunogold Labeling EM. Cells were plated in T25 flasks, rinsed in PBS, and fixed with 0.1% glutaraldehyde and 2% formaldehyde in 0.1 M phosphate buffer, pH 7.2, for 30 min at RT. In some experiments, the cells were incubated with 20 ng/ml heregulin, 10 μg/ml herceptin, or 10 ng/ml EGF in DMEM-HEPES buffer for 30 min at 4°C or 37°C (see RESULTS) before fixation. After a brief wash in PBS, the cells were incubated with mouse monoclonal anti-ErbB2 (sc-08) diluted 1:10 in PBS for 1 h at RT, rinsed in PBS, incubated with 10-nm gold-labeled goat anti-mouse (GAM-10 nm) (Amersham Biosciences AB) diluted 1:25 in PBS for 30 min at RT, and rinsed in PBS. In some experiments, cells were additionally incubated with 0.1 mg/ml protein A (Sigma-Aldrich), followed by incubation with 10 μg/ml cholera toxin B-chain (CT-B) (Sigma-Aldrich) in PBS for 1 h at RT, rinsed three times in PBS, incubated with rabbit anti-CT-B (Sigma-Aldrich) 1:800 in PBS for 1 h at RT, rinsed and incubated with 5-nm gold-labeled protein A (PAG-5 nm) (purchased from Dr. G. Posthuma, Utrecht University, Utrecht, The Netherlands) diluted 1:80 in PBS for 30 min at RT. Unspecific background of 5-nm gold, in experiments where anti-CT-B was omitted, was <1%.

The cells were then scraped off the flasks, pelleted, and postfixed in 2% OsO_4 in water, contrasted en bloc with 1% uranyl acetate, dehydrated in a graded series of ethanols, and embedded in Epon. Sections were further contrasted with lead citrate and uranyl acetate if required, and examined in a Philips CM 100 electron microscope (Philips, Eindhoven, The Netherlands).

To efficiently cross-link ErbB2, cells were incubated at either 12 or 37°C for 1 h with anti-ErbB2 antibody (sc-08) 1:100, rinsed three times, followed by GAM-10 nm diluted 1:25 for 30 min, and fixed.

Postembedding Immunogold Labeling EM. The cells were fixed with 0.1% glutaraldehyde and 2% formaldehyde in 0.1 M phosphate buffer, pH 7.2, for 30 min at RT. After fixation, cells were scraped off, sedimented for 30 min at RT, spun for 1 min in a Microfuge, and then embedded in 7.5% gelatin (Merck, Darmstadt, Germany) in PBS for 30 min at 37°C. After cooling on ice and trimming, cell pellets were infused twice for 30 min each with 2.1 and 2.3 M sucrose, respectively, mounted on aluminum stubs, and frozen in liquid nitrogen. Ultrathin sections were cut by an Ultracut S microtome (Reichert, Vienna, Austria), collected on 2.3 M sucrose in a loop, and mounted on Formvar-coated copper or nickel grids. ErbB2 proteins were detected by

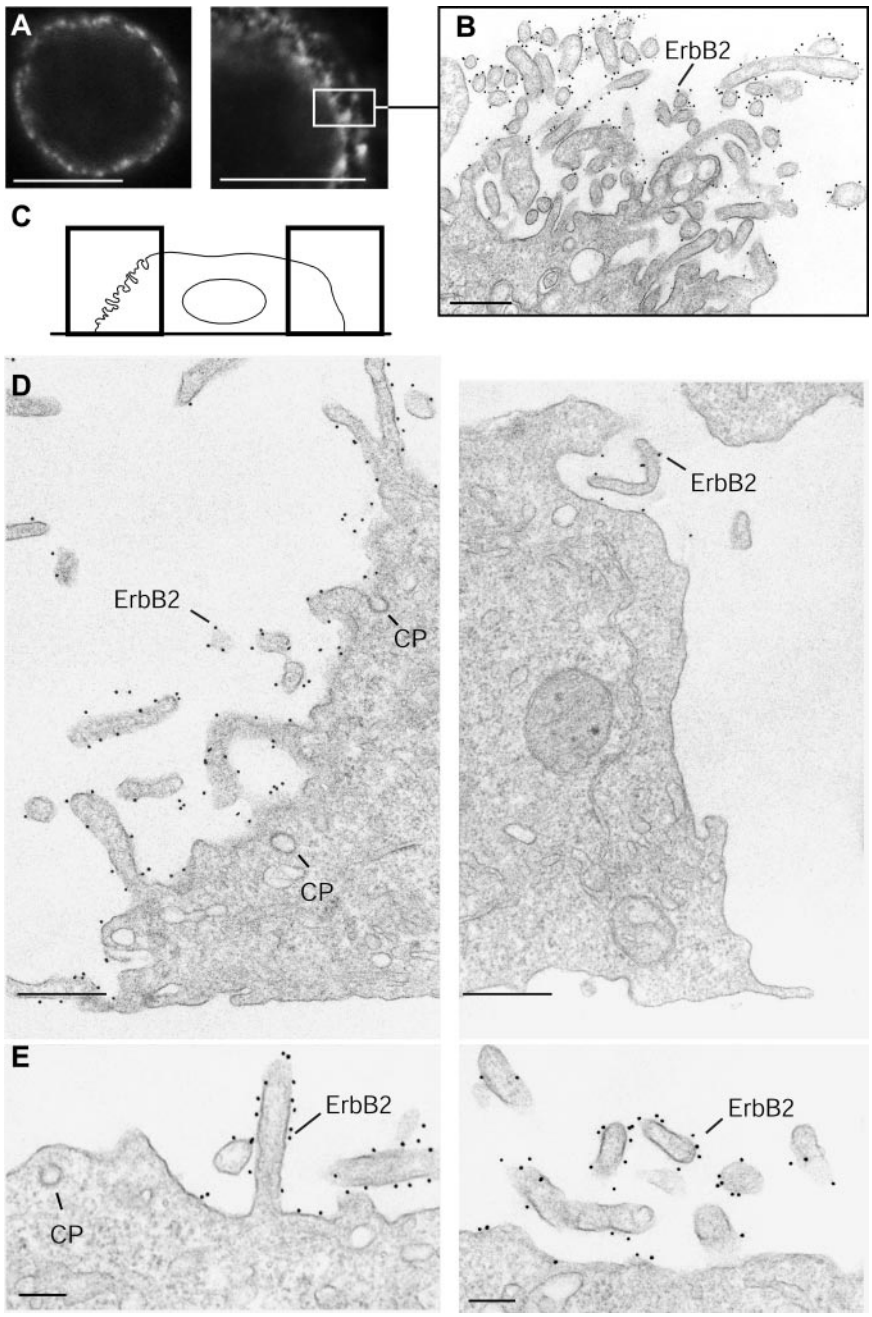

Figure 1. ErbB2 is preferentially associated with protrusions on SKBR3 cells. (A) Confocal images of fixed, permeabilized SKBR3 cells stained with the mAb Sc-08 for ErbB2. ErbB2 is present on the entire cell surface but with a very prominent, irregular staining in some regions. No intracellular labeling for ErbB2 is seen. The size of the box on the right-hand image corresponds to the EM picture in B. (C) Diagram showing how the two EM images in D are localized in relation to the entire cell. (B, D, and E) Preembedding immunogold labeling of fixed SKBR3 cells by using the Sc-08 antibody. Note that ErbB2 is preferentially associated with ruffles or protrusions of the plasma membrane, whereas the bulk membrane shows relatively low labeling. Also note that clathrin-coated pits (CP) are unlabeled. Bars, 10 μm (A), 500 nm (B and D), and 200 nm (E).

either the mouse monoclonal anti-ErbB2 (sc-08) diluted 1:10 in PBS or the rabbit polyclonal anti-ErbB2 (2242) diluted 1:10 in PBS for 1 h, followed by GAM-10 nm diluted 1:25 in PBS or PAG-5 nm diluted 1:80 for 30 min.

RESULTS

ErbB2 Is Associated with Protrusions

We used SKBR3 cells, a widely studied human breast carcinoma cell line, which in addition to a high expression level of ErbB2 also expresses EGFR and ErbB3 (Baulida and Carpenter, 1997; Wang *et al*., 1999; Nagy *et al*., 2002). To localize ErbB2 in SKBR3 cells by immunofluorescence, permeabilized cells were incubated with the mAb sc-08 against the extracellular portion of ErbB2, followed by Alexa 488-conjugated GAM (GAM-488). Confocal microscopy revealed that ErbB2 was expressed on the entire surface of SKBR3 cells, although certain regions showed a stronger, more irregular labeling (Figure 1A). To obtain a better structural resolution, immunogold surface labeling with sc-08 followed by GAM conjugated to 10-nm gold (GAM-gold) was used on prefixed, nonpermeabilized cells, which were subsequently embedded and sectioned for electron microscopy (preembedding EM). This showed that ErbB2 was very unevenly distributed on the cell surface and had a clear preference for ruffles or plasma membrane protrusions (Figure 1, B–D). The labeling density (number of gold particles per micrometer of membrane) was up to 10 times higher on such protrusions than on the nondifferentiated bulk membrane regions between the protrusions (Figure 1E).

To rule out the possibility that the surface distribution of ErbB2 as detected with sc-08 was affected by extracellular proteolysis of ErbB2, which potentially could remove the epitope recognized by sc-08, we compared Western blots with different antibodies recognizing either intracellular or extracellular epitopes (our unpublished data). In agreement with Molina *et al.* (2001), we observed virtually no cleavage of the receptor. Moreover, confocal microscopy of cells labeled with both sc-08 and the polyclonal antibody 2242 directed against the intracellular portion of ErbB2 resulted in a complete overlap of the two stains (our unpublished data). Furthermore, immunogold labeling of ultracryosections (postembedding labeling) with sc-08 or 2242 revealed gold particles exclusively on the plasma membrane, mainly on protrusions (Figure 2, A and B).

At steady state, no intracellular ErbB2 was observed by confocal microscopy. In double-labeling experiments using sc-08 or 2242 to detect ErbB2 in combination with either the polyclonal anti-TfR antibody 309i or the monoclonal anti-TfR antibody B3/25, no ErbB2 was detected in endosomes (Figure 2C). This was confirmed on ultracryosections (Figure 2, A and B). Moreover, no gold-labeling for ErbB2 was detected in clathrin-coated pits (Figures 1, D and E, and 2A). In fact, less than one of 10^4 gold particles was present in coated pits. Together, these findings suggest that the steady-state internalization rate of ErbB2 must be very low. Moreover, because clathrin-coated pits are localized to the bulk membrane between protrusions and ErbB2 is preferentially associated with protrusions, this localization of ErbB2 could explain why ErbB2 is apparently prevented from entering clathrin-coated pits.

ErbB2 Is Not Internalized in Response to EGF, heregulin, or herceptin

We next wanted to test to what extent ligand binding could influence the localization and internalization of ErbB2. Cells were treated with EGF, known to cause EGFR (ErbB1)-ErbB2 dimerization, or heregulin, a growth factor that binds to ErbB3 and ErbB4, resulting in the formation of ErbB3/4-ErbB2 dimers (Sliwkowski *et al*., 1994; Burgess *et al*., 2003), or with herceptin (trastuzumab), a humanized mAb against ErbB2. After fixation the cells were permeabilized and immunolabeled for ErbB2 with either sc-08 or 2242 in combination with the α-TfR antibodies 309i and B3/25, respec-

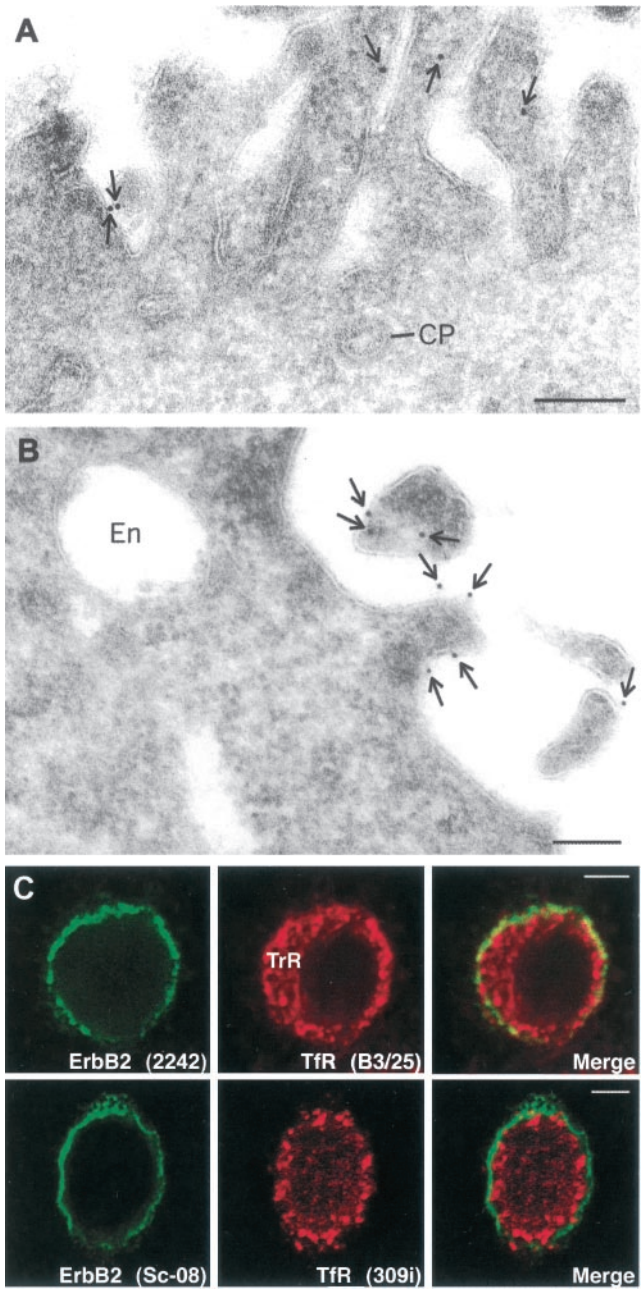

Figure 2. ErbB2 is not endocytosed in nonstimulated cells. (A and B) Immunogold detection of ErbB2 in ultracryosections of SKBR3 cells (postembedding labeling) with the polyclonal antibody 2242 against the intracellular portion of the receptor and the mAb Sc-08 against the extracellular portion of the receptor. In both cases, ErbB2 is detected on protrusions but not in clathrin-coated pits (CP) or endosomes (EN). (C) Confocal images of cells stained with 2242 or Sc-08 in combination with the monoclonal anti-TfR antibody B3/25 or the polyclonal anti-TfR antibody 309i. Note that ErbB2 is only present on the cell surface and not seen in TfR-containing endosomes. Bars, 200 nm (A and B) and 5 μm (C).

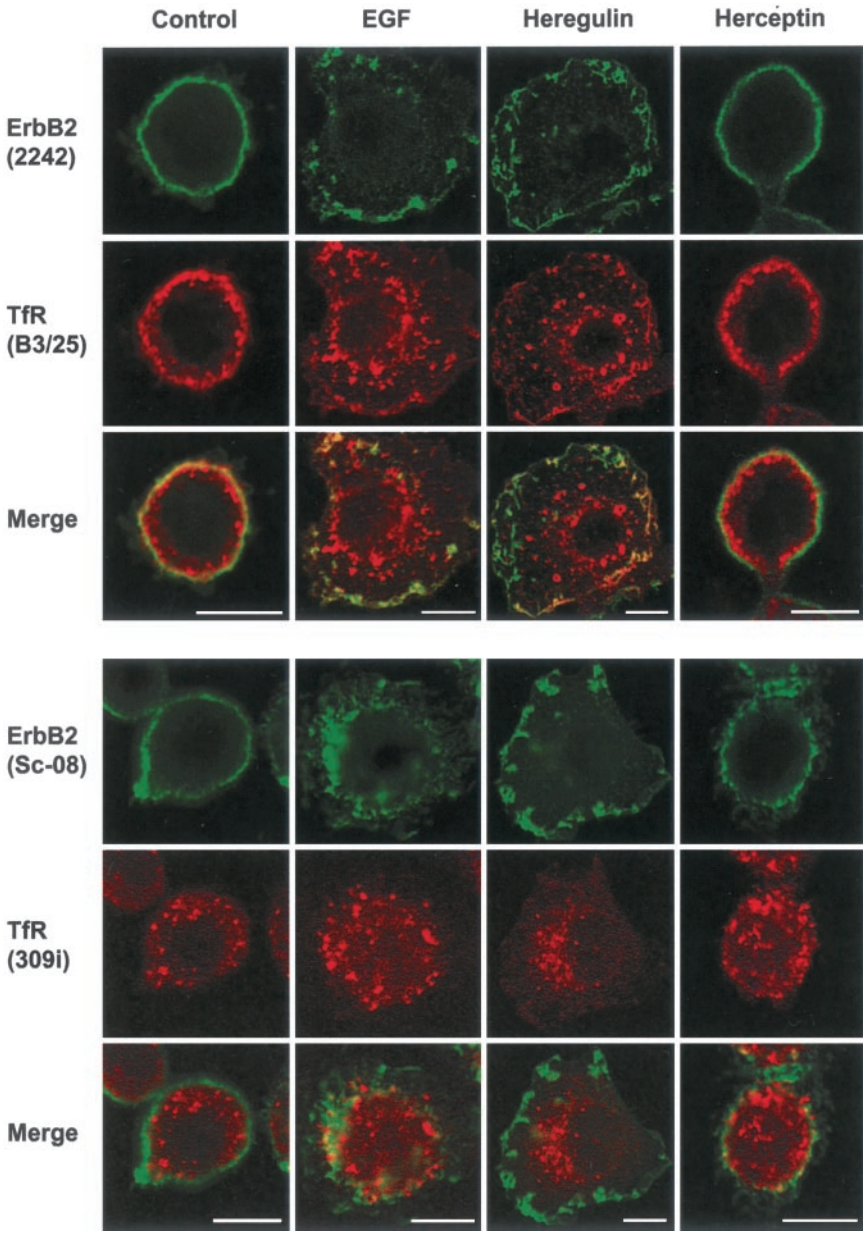

Figure 3. ErbB2 is not internalized after ligand binding. Confocal images of untreated control cells and cells treated with EGF, heregulin, or herceptin and immunolabeled for ErbB2 and the TfR as indicated. Stimulation with EGF or heregulin has pronounced effects on the cell morphology. However, in all experiments ErbB2 remains at the cell surface and does not become internalized into TfR-containing endosomes. Bar, 10 μm.

tively. Confocal microscopy showed that ErbB2 remained on the cell surface also after ligand binding and that there was no colocalization with TfR-containing endosomes (Figure 3). Both EGF and heregulin caused marked morphological changes of the SKBR3 cells; membrane ruffling or formation of protrusions became much more pronounced than seen in control cells (Figure 3). EM immunogold surface labeling showed that ErbB2 remained associated with the membrane protrusions both after binding of EGF, heregulin, and herceptin (Figure 4, A and B). Moreover, ErbB2 was still not observed in clathrin-coated pits.

To evaluate the presence of ErbB2 in endosomes by a biochemical approach, cell surface biotinylation was used. The cells were labeled with reducible sulfo-NHS-SS-Biotin. After incubation with heregulin or herceptin the biotin was stripped from the surface, the cells lysed, and the biotin precipitated with streptavidin-coated beads and the ErbB2 content, representing the internalized portion of ErbB2 during the experiment, was detected by Western blotting. In this way, a very low level of ErbB2 internalization was found after binding of heregulin or herceptin, which was similar to the steady-state level of control cells (Figure 4C). These results show that the association of ErbB2 with plasma membrane protrusions is very stable and support the notion that such stable localization to protrusions might explain the remarkable internalization resistance of ErbB2.

Localization of ErbB2 to Membrane Protrusions and Internalization Resistance Does Not Depend on Association with Rafts or the Actin Cytoskeleton

An association of ErbB2 with lipid rafts has been indicated (Mineo *et al*., 1999; Zhou and Carpenter, 2001), and recently, ErbB2 was reported to be present in caveolae, a subset of rafts, in SKBR3 cells (Nagy *et al*., 2002). Moreover, ErbB2 is also associated with the actin cytoskeleton (Adam *et al*., 1998; Brandt *et al*., 1999; Li *et al*., 1999; Feldner and Brandt,

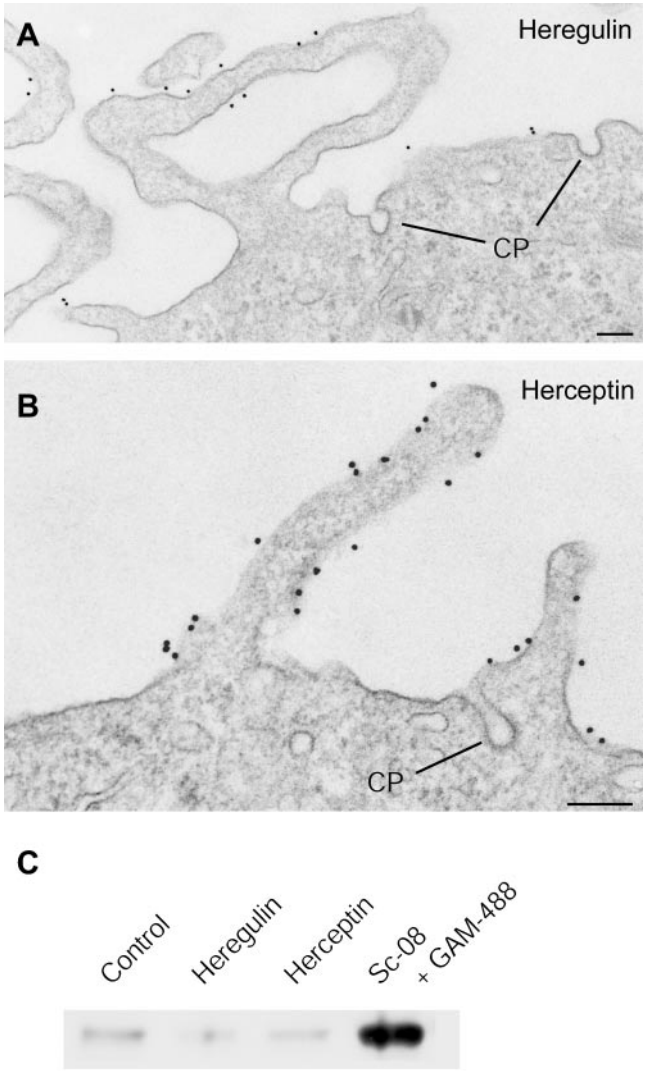

Figure 4. Ligand binding does not remove ErbB2 from protrusions or allow it to enter clathrin-coated pits and become internalized. (A and B) Immunogold labeling shows that ErbB2 is associated with protrusions of both a heregulin- (A) and a herceptin (B)-treated cell. After stimulation with herceptin, the cell surface has become highly ruffled. Note that ErbB2 is not detected in clathrin-coated pits (CP). (C) Biotinylation assay to detect internalized ErbB2. It is seen that in control cells as well as in cells treated with heregulin or herceptin, the internalization level is very low. In contrast, after antibody cross-linking, a substantial fraction of ErbB2 becomes internalized. Bars, 200 nm (A and B).

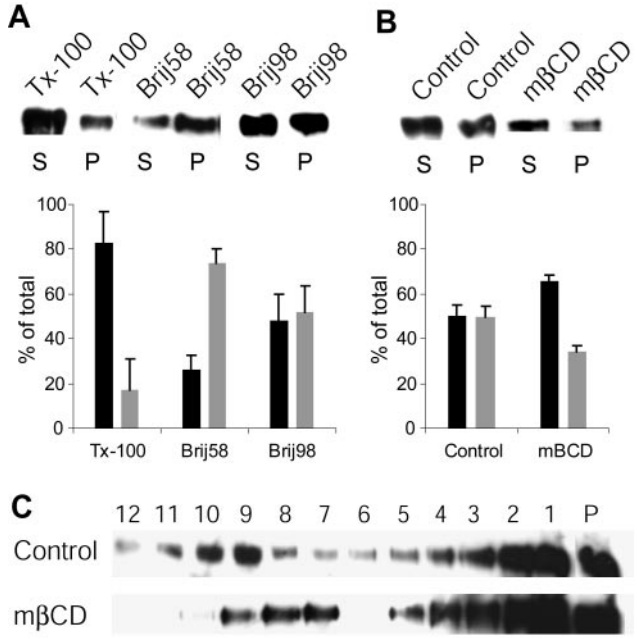

Figure 5. ErbB2 is a raft-associated receptor. (A) Western blot of ErbB2 in SKBR3 cells after detergent centrifugation by using different detergents (Tx-100, Brij58, and Brij98). S, supernatant; P, pellet. Below the blot is shown the densitometry measurements of three to five experiments for each detergent (mean ± SD). Black bars represent supernatant and gray bars pellet. (B) Western blot of ErbB2 in SKBR3 cells after cholesterol depletion with 8 mM mβCD for 30 min at 37°C with subsequent Brij98 detergent centrifugation. The densitometry measurements (of three experiments shown as mean ± SD) below show that ErbB2 is moved from the insoluble fraction (the pellet) to the soluble fraction (the supernatant) upon cyclodextrin treatment. (C) Western blots of ErbB2 with or without pretreatment of the cells with 8 mM mβCD for 30 min at 37°C followed by extraction with Brij98 at 37°C and subsequent sucrose density gradient centrifugation. It is seen that cholesterol depletion moves the low buoyancy fraction of ErbB2 down in the gradient, characteristic of raft-associated proteins.

2002). We therefore tested whether stabilization of ErbB2 by rafts, caveolae, and/or actin could explain the internalization resistance or the localization to protrusions. EM and Western blotting revealed that SKBR3 cells did not have morphologically identifiable caveolae, nor did they show any detectable expression level of caveolin-1 (our unpublished data). Next, the solubility of ErbB2 in different detergents was determined. We used Tx-100 as well as two newer, nonionic detergents of the Brij series, Brij58 and Brij98. Brij98 is a detergent with the advantageous property that it can be used at physiological temperature (Drevot *et al*., 2002; Braccia *et al*., 2003). SKBR3 cells were extracted in lysis buffer with 1% detergent, fractionated by centrifugation into supernatant and pellet, and the proteins detected by Western blotting. A fraction (~20%) of ErbB2 was found to be insoluble in Tx-100, whereas a large amount of ErbB2 (~45–75%) was insoluble in Brij98 and Brij58 (Figure 5A).

The aforementioned detergent insolubility suggested that ErbB2 is a raft-associated protein. Rafts are cholesterol-dependent microdomains (Brown and London, 2000; Simons and Toomre, 2000; Muller, 2002). Therefore, it was investigated to what extent the insoluble fraction of ErbB2 after Brij98 extraction was cholesterol dependent. Cells were incubated with the cholesterol-depleting drug mβCD for 30 min at 37°C. Cholesterol-depletion of the cells with 8 mM mβCD reduced the membrane cholesterol by ~30% (our unpublished data) and caused a shift of ErbB2 from the insoluble fraction to the soluble fraction in Brij98 detergent centrifugations (Figure 5B). The effect of mβCD was also confirmed in sucrose density gradients. After Brij98 detergent extraction, a fraction of ErbB2 floated to the low bouyancy top in the sucrose gradient, normally containing detergent-resistant membranes (Figure 5C). As expected, cholesterol depletion with mβCD caused ErbB2 to move down to higher bouyancy fractions.

To elucidate the raft localization of ErbB2 by confocal microscopy, double labeling for ErbB2 and a raft marker, the ganglioside GM1, was used. Thus, in addition to anti-ErbB2 (sc-08) and GAM-488, fixed, permeabilized cells were also

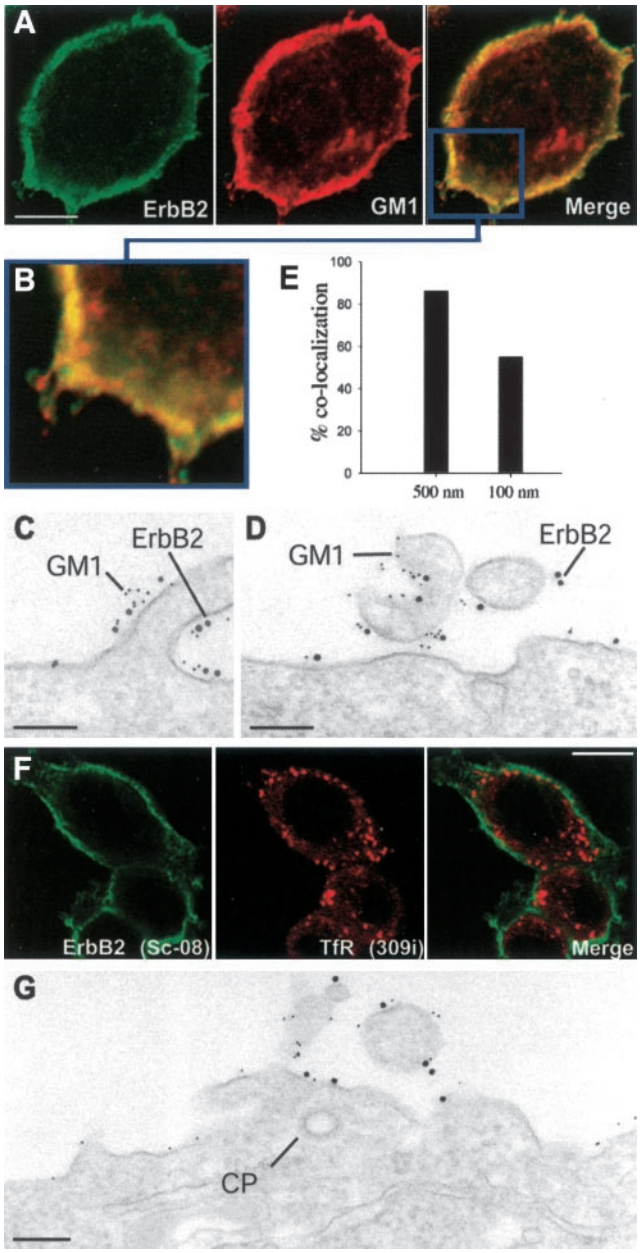

Figure 6. Cholesterol depletion does not lead to internalization of ErbB2. (A) Confocal images of an SKBR3 cell stained for ErbB2 and GM1. The merged image indicates a high degree of colocalization at the cell surface. (B) Higher magnification of a part of the merged image. (C and D) EM pictures of cells double labeled for ErbB2 (10-nm gold) and GM1 (5-nm gold). (E) Quantification of the gold labeling showing that most ErbB2 gold particles have neighboring GM1 particles both within the 500- and the 100-nm range. (F) Confocal images of cholesterol-depleted cells (mβCD) double labeled for ErbB2 and TfR. No internalized ErbB2 is observed. (G) EM immunogold double labeling for ErbB2 (10 nm) and GM1 (5 nm) of a cholesterol-depleted cell showing that ErbB2 have not been removed from the protrusions or entered clathrin-coated pits (CP). Bar, 10 μm (A), 200 nm (C and D), 10 μm (F), and 200 nm (G).

incubated with fluorescent cholera toxin B-chain (CT-594), which binds to GM1. Confocal microscopy indicated a high degree of colocalization between ErbB2 and GM1 (Figure 6, A and B). However, a higher resolution is required to eliminate problems with superimposition of separate domains at the irregular surface of SKBR3 cells. We therefore used EM immunogold double labeling for ErbB2 and cholera toxin B-chain bound to GM1. This revealed that ErbB2 and GM1 were often very close to each other, not least on protrusions (Figure 6, C and D). A quantification of gold particles showed that >80% of the ErbB2 gold particles were <500 nm away from GM1 gold particles, and ~60% of the ErbB2 golds were <100 nm away from GM1 golds (Figure 6E). Importantly, after cholesterol depletion with mβCD, ErbB2 remained at the plasma membrane and could not be detected in TfR-containing endosomes, as revealed by confocal microscopy (Figure 6F). Moreover, EM immunogold labeling showed that ErbB2 still had a preference for protrusions and that it had no access to clathrin-coated pits (Figure 6G).

To study the effect of disrupted actin cytoskeleton on ErbB2 localization and internalization, cells were treated with latrunculin and subsequently extracted with Brij98. As seen in Figure 7A, whereas actin was equally distributed between supernatant and pellet after detergent centrifugation of control cells, latrunculin shifted all actin to the supernatant. In contrast, the distribution of ErbB2 between the pellet fraction and the supernatant was comparably unaffected. EM showed pronounced morphological changes of the cell cortex after disruption of the actin cytoskeleton with latrunculin. The entire cell surface became highly irregular, presumably because of the normally stabilizing, cortical actin cytoskeleton was destroyed, so that a clear distinction between protrusions and bulk membrane was not possible (Figure 7, B and C). In agreement with other studies of the relation between the actin cytoskeleton and the clathrin-mediated endocytosis (Gaidarov *et al*., 1999; Cao *et al*., 2003; da Costa *et al*., 2003), the number of clathrin-coated pits increased considerable. Most importantly, immunogold labeling did not reveal any ErbB2 in the coated pits (Figure 7, B and C).

Together, these results strongly indicate that ErbB2's preference for protrusions and lack of affinity for clathrin-coated pits is not due to association of ErbB2 with either rafts or the actin cytoskeleton.

Extensive Cross-linking of ErbB2 Removes the Receptor from Protrusions and Leads to Internalization

Only after extensive cross-linking of ErbB2, that is, after incubating live cells with sc-08 followed by GAM-gold or GAM-488, a marked internalization was noticed. The biotinylation assay showed a high internalization level of ErbB2 after such cross-linking (Figure 4C). Moreover, in EM experiments (using GAM-10 nm), it was clear that after cross-linking at 12°C, ErbB2 was efficiently removed from the protrusions and concentrated on the bulk membrane, including clathrin-coated pits (Figure 8A). At 37°C ErbB2 gold labeling was still present at the cell surface, but it was in particular concentrated in endosomes (Figure 8B). These endosomes often occurred as multivesicular bodies and tended to form aggregates (Figure 8B). Similarly, in confocal microscopy experiments with sc-08 against ErbB2 and 309i against the TfR, cross-linking resulted in removal of ErbB2 from the cell surface and a marked colocalization of ErbB2 with the TfR in endosomes (Figure 9). These findings further support a correlation between the preferential localization of ErbB2 to protrusions and the lack of the receptor in coated pits, and subsequently in endosomes.

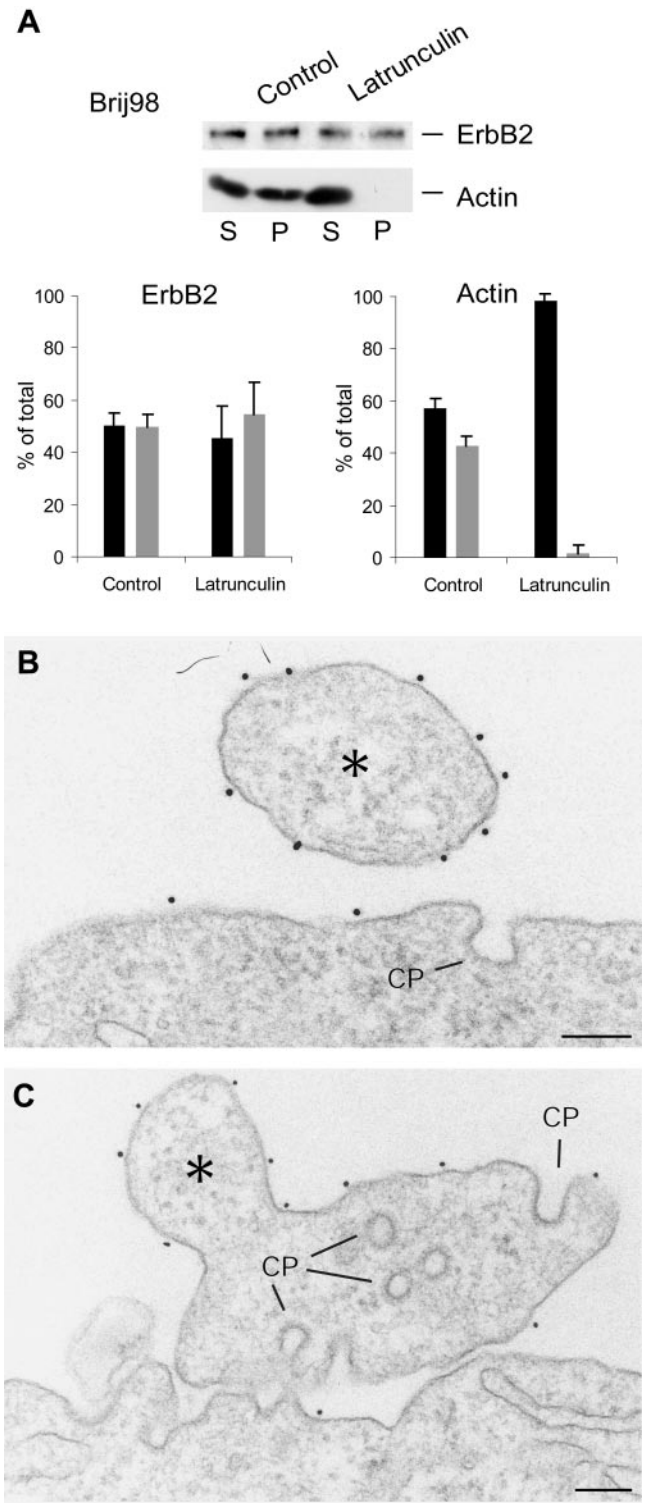

Figure 7. Actin depolymerization does not allow ErbB2 to enter clathrin-coated pits. (A) Western blot of actin and ErbB2 in SKBR3 cells after incubation with latrunculin and detergent centrifugation with Brij98. S, supernatant; P, pellet. Below the blot is shown densitometry measurements of three experiments (mean ± SD). Black bars represent supernatant, and gray bars pellet. Actin is shifted completely to the supernatant fraction, whereas ErbB2 is unaffected. (B and C) EM pictures of latrunculin-treated cells labeled for ErbB2. Note that ErbB2 is still concentrated on protrusion-like structures (asterisks) at the highly irregular cell surface and that the clathrin-coated pits (CP) are unlabeled. Bars, 200 nm (B and C).

DISCUSSION

Whether ErbB2 is a recycling receptor or an internalization-resistant receptor has been debated for a long time. The present results show that in the ErbB2-overexpressing human breast carcinoma cell line SKBR3, ErbB2 has a pronounced preference for plasma membrane ruffles or protrusions. Moreover, it is very efficiently excluded from clathrin-coated pits, and it is not delivered to recycling endosomes, even after treating the cells with EGF, heregulin, or herceptin. However, extensive cross-linking of ErbB2 can remove it from the protrusions and direct it to clathrin-coated pits and into endosomes. These findings indicate a correlation between the stable association with protrusions and the internalization resistance.

After ligand binding the EGFR (ErbB1) is rapidly downregulated by a ubiquitin-cCbl mediated pathway through endosomes to lysosomes. In contrast, it is widely accepted that ErbB2 removes its dimerization partners from this pathway and instead allows efficient recycling from endosomes to the cell surface (Lenferink *et al.*, 1998; Yarden, 2001). This implies that it should be possible to localize ErbB2 to clathrin-coated pits and that ErbB2 exists in an equilibrium between the plasma membrane and endosomes, implications that are not supported by the present findings. However, our results are in line with previous reports showing that ErbB2 is not efficiently endocytosed (Baulida *et al.*, 1996; Wang *et al.*, 1999). Baulida *et al.* (1996) showed that ErbB2 is poorly internalized in response to ligand treatment and activation. However, because ErbB2 has no specific ligand, Baulida *et al.* (1996) used ErbB chimeras made of N-terminal ERFR and C-terminal ErbB2, -3, or -4 to bind ^{125}I-EGF. Several studies of ErbB internalization are based on binding of radiolabeled ligand and compare the amount of internalized probe to the amount of total bound probe. This assumes that the entire receptor population is readily accessible for the ligand. However, it has been shown that only a subset of the EGFR population is available for efficient EGF binding and that the size of this population depends on lipid rafts (Roepstorff *et al.*, 2002). Thus, the internalization ratio observed with ligand binding studies might not reflect the actual degree of internalization.

One of the best-studied internalization and recycling receptors is the TfR. Clathrin-coated pits constitute ~1–1.5% of the cell surface area, which means that ~1–1.5% of a resident membrane protein without an internalization signal should be found in clathrin-coated pits, whereas ~10% of the TfR are found in coated pits (Hansen *et al.*, 1992). This corresponds to a six- to ninefold concentration of TfRs in coated pits. This efficient concentration is mediated by the YXXΦ motif positioned close to the transmembrane domain. Because $<0.1°/_{oo}$ of ErbB2 was found in clathrin-coated pits, this receptor does not only lack a signal for coated pits, but it is excluded from the pits by a factor of 100 or more. Such an exclusion cannot be explained by lack of an internalization signal only (Sorkin *et al.*, 1993) but requires a signal or a protein–protein interaction actively keeping ErbB2 away from coated pits. We speculate that this is the same signal or interaction that mediates the preferential localization of ErbB2 to protrusions. It should be mentioned, however, that clathrin-independent endocytic mechanisms exist (Sandvig and van Deurs, 2002) and recent results indicated that the EGFR may be internalized by a clathrin-independent mechanism (Hinrichsen *et al.*, 2003). In any case, internalization of ErbB2 is very limited.

The concept that ErbB2 becomes internalized derives at least in part from previous EM studies using gold-conju-

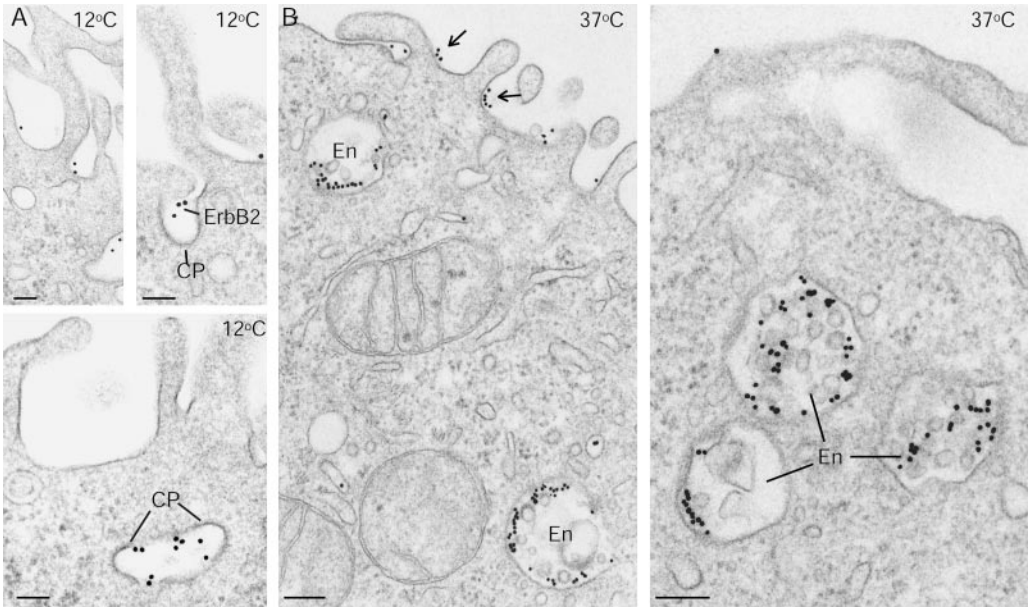

Figure 8. Cross-linking of ErbB2 with Sc-08 followed by GAM-gold on live cells removes ErbB2 from protrusions, causes it to enter clathrin-coated pits, and to reach endosomes. (A) At 12°C, ErbB2 is no longer present on the protrusions but is seen in clathrin-coated pits (CP). (B) At 37°C, some ErbB2 may still be present on the bulk membrane between protrusions (arrows), although most is now found in endosomes (EN). Note that the endosomes occur as multivesicular bodies and that they form clusters (right-hand image). Bars, 100 nm (A) and 200 nm (B).

gated anti-ErbB2 antibodies (Maier *et al*., 1991; Hurwitz *et al*., 1995). In this way, it was shown that gold particles initially were present on the cell surface and in clathrin-coated pits and later on also in endosomes, multivesicular bodies and lysosomes, much like other receptors known to be internalized. This was also what we found using receptor cross-linking. However, the behavior of gold-conjugated antibodies which cross-link receptors do not reflect the correct localization and trafficking of the native receptor. For this purpose, one should detect the receptor on fixed, intact cells or on thawed ultracryosections as reported here, and by this approach ErbB2 was not detectable in coated pits and endosomes.

Our results suggested that the stable association of ErbB2 with protrusions was not due to retention in rafts or anchoring by the actin cytoskeleton. Raft association of a protein is often defined based on insolubility in cold Tx-100 (Brown and Rose, 1992; Simons and Ikonen, 1997; Simons and Toomre, 2000). However, Tx-100 may artifactually stimulate formation of lipid rafts (Heerklotz, 2002), and recently attention has been paid to other nonionic, "milder" detergents such as Lubrol WX and the Brij series (Brij58 and 98). In particular, Brij98 has the advantage that it can be used at 37°C where it reveals insolubility of several liquid-ordered membrane components such as sphingomyelins and GPI-anchored, -palmitoylated, and -myristoylated proteins (Drevot *et al*., 2002; Braccia *et al*., 2003). From our results, it is clear that only a proportion of ErbB2 is raft-associated, and we hypothesize that ErbB2 in the steady-state situation exists in a dynamic equilibrium with rafts in the protrusion membrane so that, at a given time point, only a fraction of ErbB2 is directly interacting with the raft gangliosides. This transient ErbB2–ganglioside interaction is cholesterol dependent and could potentially regulate the function of ErbB2 (heterodimerization, ligand binding, and signaling), in agreement with the concept that gangliosides actively regulate growth factor receptor activity (Miljan and Bremer, 2002). We recently found that cholesterol depletion and subsequent release of the EGFR from rafts increased EGF binding to this receptor, indicating that raft association may have a negative regulatory role on EGFR activity (Roepstorff *et al*., 2002). For ErbB2, this may not be true. Binding of heregulin and herceptin did not change the affinity of ErbB2 to rafts (our unpublished data). Thus, the significance of the ErbB2–raft interaction remains unclear. However, what is clear is that cholesterol depletion and subsequent perturbation of rafts did not remove ErbB2 from protrusions or allowed the receptor to enter clathrin-coated pits. It is well-established that ErbB2 is involved in reorganizing the actin cytoskeleton during migration and metastasis (Adam *et al*., 1998; Brandt *et al*., 1999; Chausovsky *et al*., 2000; Feldner and Brandt, 2002). Moreover, it has been reported that ErbB2 is part of a glycoprotein complex that binds to actin microfilaments, although ErbB2 itself was not directly associated with actin (Li *et al*., 1999). However, even after severe perturbation of the actin cytoskeleton by latrunculin, we did not observe ErbB2 in clathrin-coated pits. Thus, we propose that the internalization resistance of ErbB2 is not due to a direct binding of ErbB2 to the actin cytoskeleton.

Herceptin, a widely used drug in the treatment of breast cancer, is generally believed to perturb the recycling pathway followed by ErbB2 and instead cause transport to lysosomes and receptor down-regulation (Rubin and Yarden, 2001; Yarden, 2001; Menard *et al*., 2003). Other possible effects of herceptin that do not require ErbB2 internalization have also been suggested; for instance, that herceptin prevents dimerization (Klapper *et al*., 1997) or extracellular proteolysis of ErbB2 that can make the receptor constitutively active (Molina *et al*., 2001). This proteolytic activity takes place in vivo, but Molina *et al.* (2001) also carried out an in vitro experiment with SKBR3 cells showing that extracellular cleavage of ErbB2 did not take place on SKBR3 cells unless a metalloprotease activator was added to the medium. Importantly, this induced proteolysis could be coun-

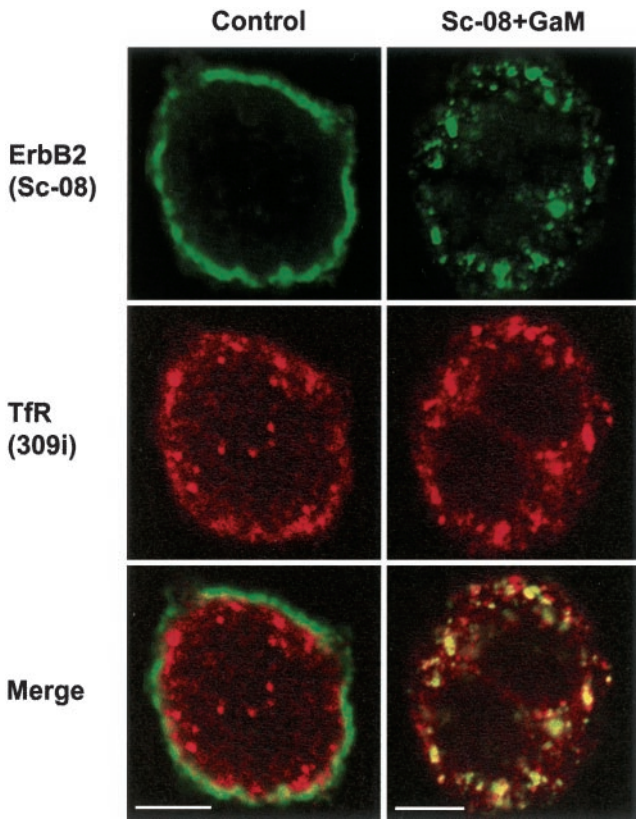

Figure 9. Cross-linking causes internalization of ErbB2 into TfR-containing endosomes. Confocal images of a control cell and a cell on which ErbB2 was cross-linked with Sc-08 followed by GAM-488 before fixation. Bar, 5 μm.

teracted by adding herceptin. Our results support the possibility of alternative mechanisms of herceptin action, because ErbB2 persists on the protrusions after herceptin treatment and is not detected in endosomes. This is in contrast to the general perception of an increased internalization and degradation of ErbB2 caused by the drug.

In conclusion, ErbB2 is an internalization-resistant receptor stably associated with membrane protrusions. Future research should reveal the biological importance of this association as well as characterize the signal or protein interaction, which apparently causes this association as well as the exclusion from clathrin-coated pits and subsequent down-regulation of ErbB2.

ACKNOWLEDGMENTS

We thank Ulla Hjortenberg and Mette Ohlsen for expert technical assistance and Keld Ottesen for photographical work. We thank Kirstine Roepstorff, Frederik Vilhardt, and Michael Grandal in the laboratory for valuable discussions. We also thank Professor M. Rörth for providing herceptin. This study was supported by grants from the Danish Cancer Society, the Danish Medical Research Counsil, the Novo Nordic Foundation, and the John and Birthe Meyer Foundation.

REFERENCES

Adam, L., Vadlamudi, R., Kondapaka, S.B., Chernoff, J., Mendelsohn, J., and Kumar, R. (1998). Heregulin regulates cytoskeletal reorganization and cell migration through the p21-activated kinase-1 via phosphatidylinositol-3 kinase. J. Biol. Chem. *273*, 28238–28246.

Baulida, J., and Carpenter, G. (1997). Heregulin degradation in the absence of rapid receptor-mediated internalization Exp. Cell Res. *232*, 167–172.

Baulida, J., Kraus, M.H., Alimandi, M., Di Fiore, P.P., and Carpenter, G. (1996). All ErbB receptors other than the epidermal growth factor receptor are endocytosis impaired. J. Biol. Chem. *271*, 5251–5257.

Braccia, A., Villani, M., Immerdal, L., Niels-Christiansen, L.L., Nystrom, B.T., Hansen, G.H., and Danielsen, E.M. (2003). Microvillar membrane microdomains exist at physiological temperature: galectin-4's role as lipid raft stabilizer revealed by 'superrafts'. J. Biol. Chem. *19*, 19.

Brandt, B.H., *et al.* (1999). c-erbB-2/EGFR as dominant heterodimerization partners determine a motogenic phenotype in human breast cancer cells. FASEB J. *13*, 1939–1949.

Brown, D.A., and London, E. (2000). Structure and function of sphingolipid- and cholesterol-rich membrane rafts. J. Biol. Chem. *275*, 17221–17224.

Brown, D.A., and Rose, J.K. (1992). Sorting of GPI-anchored proteins to glycolipid-enriched membrane subdomains during transport to the apical cell surface. Cell *68*, 533–544.

Burgess, A.W., *et al.* (2003). An open-and-shut case? Recent insights into the activation of EGF/ErbB receptors. Mol. Cell *12*, 541–552.

Cao, H., Orth, J.D., Chen, J., Weller, S.G., Heuser, J.E., and McNiven, M.A. (2003). Cortactin is a component of clathrin-coated pits and participate in receptor-mediated endocytosis. Mol. Cell. Biol. *23*, 2162–2170.

Chausovsky, A., Waterman, H., Elbaum, M., Yarden, Y., Geiger, B., and Bershadsky, A.D. (2000). Molecular requirements for the effect of neuregulin on cell spreading, motility and colony organization. Oncogene *19*, 878–888.

Citri, A., Skaria, K.B., and Yarden, Y. (2003). The deaf and the dumb: the biology of ErbB-2 and ErbB-3. Exp Cell Res. *284*, 54–65.

da Costa, S. R., *et al.* (2003). Impairing actin filament or syndapin functions promotes accumulation of clathrin-coated vesicles at the apical plasma membrane of acinar epithelial cells. Mol. Biol. Cell *14*, 4397–4413.

Drevot, P., Langlet, C., Guo, X.J., Bernard, A.M., Colard, O., Chauvin, J.P., Lasserre, R., and He, H.T. (2002). TCR signal initiation machinery is preassembled and activated in a subset of membrane rafts. EMBO J. *21*, 1899–1908.

Eccles, S.A. (2001). The role of c-erbB-2/HER2/neu in breast cancer progression and metastasis. J. Mammary Gland Biol. Neoplasia *6*, 393–406.

Feldner, J.C., and Brandt, B.H. (2002). Cancer cell motility–on the road from c-erbB-2 receptor steered signaling to actin reorganization. Exp. Cell Res. *272*, 93–108.

Gaidarov, I., Santini, F., Warren, R.A., and Keen, J.H. (1999). Spatial control of coated-pit dynamics in living cells. Nat. Cell Biol. *1*, 1–7.

Gilboa, L., Ben-Levy, R., Yarden, Y., and Henis, Y.I. (1995). Roles for a cytoplasmic tyrosine and tyrosine kinase activity in the interactions of Neu receptors with coated pits. J. Biol. Chem. *270*, 7061–7067.

Hansen, S.H., Sandvig, K., and van Deurs, B. (1992). Internalization efficiency of the transferrin receptor. Exp. Cell Res. *199*, 19–28.

Heerklotz, H. (2002). Triton promotes domain formation in lipid raft mixtures. Biophys. J. *83*, 2693–2701.

Hendriks, B.S., Opresko, L.K., Wiley, H.S., and Lauffenburger, D. (2003a). Coregulation of epidermal growth factor receptor/human epidermal growth factor receptor 2 (HER2) levels and locations: quantitative analysis of HER2 overexpression effects. Cancer Res. *63*, 1130–1137.

Hendriks, B.S., Opresko, L.K., Wiley, H.S., and Lauffenburger, D.A. (2003b). Quantitative analysis of HER2-mediated effects on HER2 and EGFR endocytosis: distribution of homo- and heterodimers depends on relative HER2 levels. J. Biol. Chem. 278, 243343–243351.

Hinrichsen, L., Harborth, J., Andrees, L., Weber, K., and Ungewickell, E.J. (2003). Effect of clathrin heavy chain- and alpha-adaptin-specific small inhibitory RNAs on endocytic accessory proteins and receptor trafficking in HeLa cells. J. Biol. Chem. *278*, 45160–45170.

Hurwitz, E., Stancovski, I., Sela, M., and Yarden, Y. (1995). Suppression and promotion of tumor growth by monoclonal antibodies to ErbB-2 differentially correlate with cellular uptake. Proc. Natl. Acad. Sci. USA *92*, 3353–3357.

Klapper, L.N., Vaisman, N., Hurwitz, E., Pinkas-Kramarski, R., Yarden, Y., and Sela, M. (1997). A subclass of tumor-inhibitory monoclonal antibodies to ErbB-2/HER2 blocks crosstalk with growth factor receptors. Oncogene *14*, 2099–2109.

Klapper, L.N., Waterman, H., Sela, M., and Yarden, Y. (2000). Tumor-inhibitory antibodies to HER-2/ErbB-2 may act by recruiting c-Cbl and enhancing ubiquitination of HER-2. Cancer Res. *60*, 3384–3388.

Lenferink, A.E.G., *et al.* (1998). Differential endocytic routing of homo- and hetero-dimeric ErbB tyrosine kinases confers signaling superiority to receptor heterodimers. EMBO J. *17*, 3385–3397.

Li, Y., Hua, F., Carraway, K.L., and Carraway, C.A. (1999). The p185(neu)-containing glycoprotein complex of a microfilament-associated signal transduction particle. Purification, reconstitution, and molecular associations with p58(gag) and actin. J. Biol. Chem. *274*, 25651–25658.

Maier, L.A., Xu, F.J., Hester, S., Boyer, C.M., McKenzie, S., Bruskin, A.M., Argon, Y., and Bast, R.C., Jr. (1991). Requirements for the internalization of a murine monoclonal antibody directed against the HER-2/neu gene product c-erbB-2. Cancer Res. *51*, 5361–5369.

Menard, S., Pupa, S.M., Campiglio, M., and Tagliabue, E. (2003). Biologic and therapeutic role of HER2 in cancer. Oncogene. *22*, 6570–6578.

Miljan, E.A., and Bremer, E.G. (2002). Regulation of growth factor receptors by gangliosides. Science' STKE *2002*. Available online at www.stke.org/cgi/content/full/sigtrans;2002/160/re15.

Mineo, C., Gill, G.N., and Anderson, R.G.W. (1999). Regulated Migration of Epidermal Growth Factor Receptor from Caveolae. J. Biol. Chem. *274*, 30636–30643.

Molina, M.A., Codony-Servat, J., Albanell, J., Rojo, F., Arribas, J., and Baselga, J. (2001). trastuzumab (herceptin), a humanized anti-Her2 receptor monoclonal antibody, inhibits basal and activated Her2 ectodomain cleavage in breast cancer cells. Cancer Res. *61*, 4744–4749.

Muller, G. (2002). Dynamics of plasma membrane microdomains and cross-talk to the insulin signalling cascade. FEBS Lett. *531*, 81–87.

Nagy, P., Vereb, G., Sebestyen, Z., Horvath, G., Lockett, S.J., Damjanovich, S., Park, J.W., Jovin, T.M., and Szollosi, J. (2002). Lipid rafts and the local density of ErbB proteins influence the biological role of homo- and heteroassociations of ErbB2. J. Cell Sci. *115*, 4251–4262.

Reese, D.M., and Slamon, D.J. (1997). HER-2/neu signal transduction in human breast and ovarian cancer stem cells. *15*, 1–8.

Roepstorff, K., Thomsen, P., Sandvig, K., and van Deurs, B. (2002). Sequestration of EGF receptors in non-caveolar lipid rafts inhibits ligand binding. J. Biol. Chem. *277*, 18954–18960.

Rubin, I., and Yarden, Y. (2001). The basic biology of HER2. Ann. Oncol. *12*, S3–S8.

Sandvig, K., and van Deurs, B. (2002). Membrane traffic exploited by protein toxins. Annu. Rev. Cell Dev. Biol. *18*, 1–24.

Simons, K., and Ikonen, E. (1997). Functional rafts in cell membranes. Nature *387*, 569–572.

Simons, K., and Toomre, D. (2000). Lipid rafts and signal transduction. Nat. Rev. Mol. Cell. Biol. *1*, 31–39.

Slamon, D.J., *et al.* (1989). Studies of the HER-2/neu proto-oncogene in human breast and ovarian cancer Science *244*, 707–712.

Sliwkowski, M.X., *et al.* (1994). Coexpression of erbB2 and erbB3 proteins reconstitutes a high affinity receptor for heregulin. J. Biol. Chem. *269*, 14661–14665.

Sorkin, A., Di Fiore, P.P., and Carpenter, G. (1993). The carboxyl terminus of epidermal growth factor receptor/erbB-2 chimerae is internalization impaired. Oncogene *8*, 3021–3028.

Sorkin, A., and Von Zastrow, M. (2002). Signal transduction and endocytosis: close encounters of many kinds. Nat. Rev. Mol. Cell. Biol. *3*, 600–614.

Wang, Z., Zhang, L., Yeung, T.K., and Chen, X. (1999). Endocytosis deficiency of epidermal growth factor (EGF) receptor-ErbB2 heterodimers in response to EGF stimulation. Mol. Biol. Cell *10*, 1621–1636.

Waterman, H., Sabanai, I., Geiger, B., and Yarden, Y. (1998). Alternative intracellular routing of ErbB receptors may determine signaling potency. J. Biol. Chem. *273*, 13819–13827.

Yarden, Y. (2001). Biology of HER2 and its importance in breast cancer. Oncology. *61*, 1–13.

Yarden, Y., and Sliwkowski, M.X. (2001). Untangling the ErbB signalling network. Nat. Rev. Mol. Cell. Biol. *2*, 127–137.

Zhou, W., and Carpenter, G. (2001). Heregulin-dependent translocation and hyperphosphorylation of ErbB-2. Oncogene. *20*, 3918–3920.